Solvent exchange rates of side-chain amide protons in proteins

Ponni Rajagopal, Bryan E. Jones & Rachel E. Klevit*
Department of Biochemistry, Biomolecular Structure Center, Box 357742,
University of Washington, Seattle, WA 98195-7742, U.S.A.

Abstract

Solvent exchange rates and temperature coefficients for Asn/Gln side-chain amide protons have been measured in *Escherichia coli* HPr. The protons of the eight side-chain amide groups (two Asn and six Gln) exhibit varying exchange rates which are slower than some of the fast exchanging backbone amide protons. Differences in exchange rates of the E and Z protons of the same side-chain amide group are obtained by measuring exchange rates at pH values > 8. An NOE between a side-chain amide proton and a bound water molecule was also observed.

Abbreviations: E. coli; *Escherichia coli*, HPr, histidine-containing phospho-carrier protein.

Participation of the side chains of asparagine, glutamine, and arginine in hydrogen bonds has been inferred from many high resolution crystal structures. The ability to detect the existence of such interactions in solution would be useful in the study of protein structure, protein stability, and protein interactions. We therefore have attempted to measure properties of side-chain amide groups that can highlight their important structural roles.

The solvent exchange rates of slowly exchanging backbone amide protons from H-D exchange experiments have been characterized for many proteins in solution. There is reasonably good correlation between protection from solvent exchange and participation in hydrogen bonds in slowly exchanging amide protons. The intrinsic solvent exchange rates of backbone and side-chain amide protons are essentially the same (Wüthrich and Wagner, 1979). However, it is extremely unusual to observe the resonances of side-chain amide groups in the first time point of an H-D exchange experiment. This indicates that the exchange lifetimes are less than ∼5 min. Measurement of shorter exchange lifetimes requires somewhat more complicated experimental techniques.

Solvent exchange rates of Gln and Asn side-chain amide protons in model amino acids and model peptides have been measured using saturation recovery methods (Krishna et al., 1982; Narutis and Kopple, 1983; Bai et al., 1993). The exchange rate of a Gln side-chain amide proton in a detergent-solubilized membrane protein was measured and found to be the same as in a model peptide (O'Neil and Sykes, 1989). Two hydrogen-bonded side-chain amide groups in BPTI have been shown to have considerably reduced exchange rates (Tüchsen and Woodward, 1987). To our knowledge, a complete and comparative analysis of the backbone and Gln/Asn side-chain amide proton exchange rates within a protein has not been reported. Such information can serve as a foundation for studies involving intermolecular interactions. We have therefore measured solvent exchange rates of the side-chain amide groups in *Escherichia coli* HPr, a protein which is a part of the bacterial sugar transport cascade. *E. coli* HPr (9 kDa; 85 residues) has six Gln and two Asn residues, some of which experience significant changes (more than the backbone) upon complexation with enzyme IIA[glc], another protein in the phosphorylation cascade (Rajagopal and Klevit, 1994; unpublished observations). These significant changes include chemical shift, solvent exchange

---

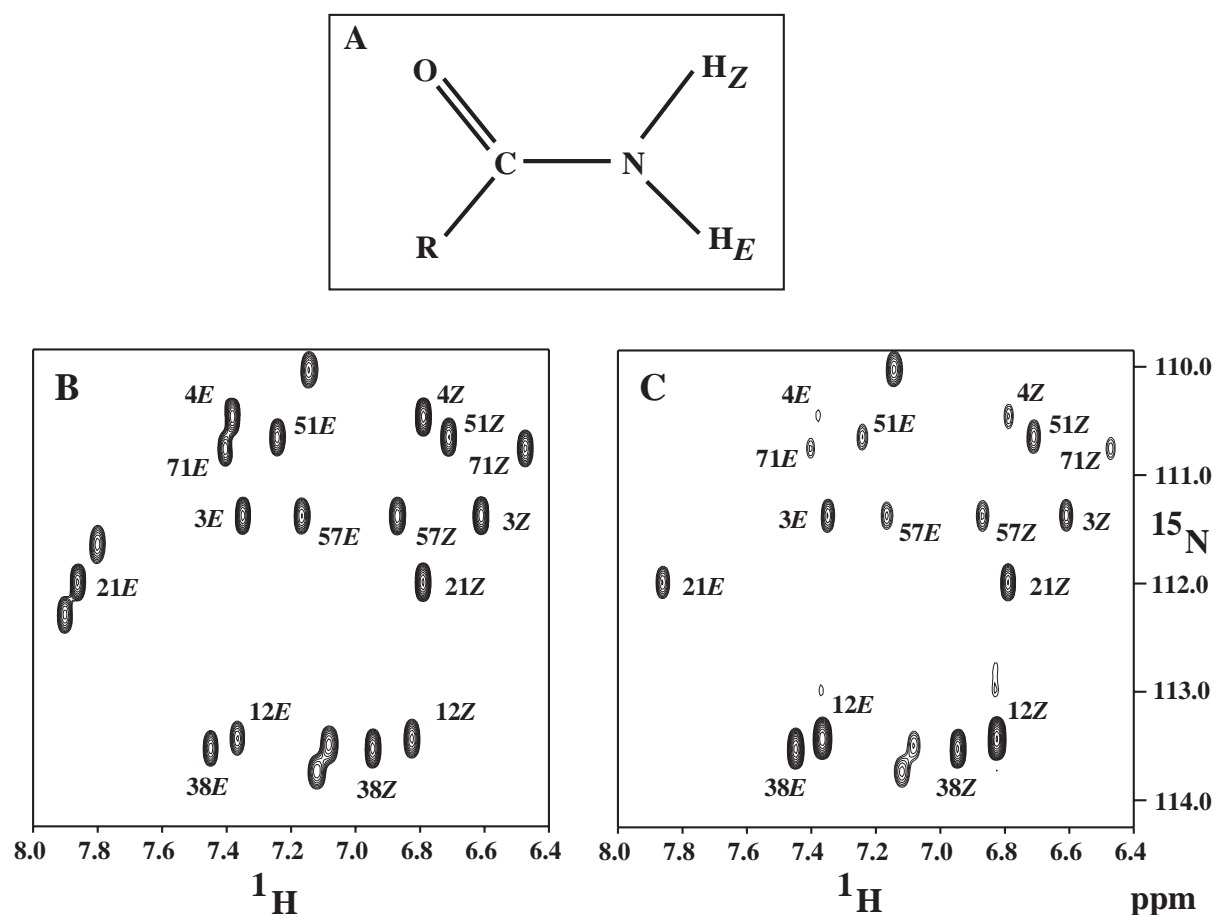* To whom correspondence should be addressed.

Figure 1. (A) A schematic of an Asn/Gln side-chain showing the orientation of the primary amide NH_2 with respect to the carbonyl oxygen. The H_E proton is *anti* to the carbonyl oxygen and the H_Z proton is *syn* to the carbonyl oxygen. (B) A region of the ^{1}H-^{15}N flip-back HSQC spectrum showing the side-chain amide groups in HPr. The spectrum was collected on a Bruker DMX 500 spectrometer equipped with a triple resonance probehead and triple-axis gradients, at pH 7.4 and 25 °C on a 1 mM sample of HPr in a 90% H_2O/10% D_2O solution containing 80 mM potassium phosphate, 40 mM KCl, 2.0 mM $MgCl_2$ and 100 μM EDTA. The spectrum was acquired with 100 (t_1) × 512 (t_2) complex points and spectral widths of 1520 Hz (F1) and 7002.8 Hz (F2). Thirty-two scans were acquired per complex t_1, point. (C) The water-NOESY difference spectrum showing the primary amide NH_2 region in HPr. The spectrum was collected on the same sample under the same conditions as in (B). The difference spectrum was obtained from two interleaved datasets collected with 100 (t_1) × 512 (t_2) complex points. The relaxation delay between scans was set to 3.0 s. During this delay, the amide protons had recovered to 99% of their equilibrium magnetization and the water magnetization had recovered to 95% of its equilibrium value. A NOESY mixing time of 100 ms was used. The rest of the parameters were the same as in (B). The spectra in (B) and (C) were zero-filled in both dimensions to 2K and apodized with a sine-bell square shifted by 90 °C with the data value set to one for the first 200 points. In both panels (B) and (C), the E and the Z protons of the Asn/Gln side-chain groups are marked with residue number. The data were processed and analyzed on a Silicon Graphics workstation with NMRPipe (Delaglio et al., 1995) and PIPP (Garrett et al., 1991). In panel C, intense difference peaks are observed for the Asn[12] and Asn[38], E and Z protons, indicating large solvent exchange rates. Differential exchange peak intensities are also observed within a side-chain amide group, viz., 51E versus 5IZ. The faint cross peaks observed at the resonance positions of 12E and 12Z displaced upfield in the ^{15}N dimension, are due to the ^{15}NHD group.

rates, and intermolecular N0Es. *E. coli* HPr has been assigned and high resolution NMR and X-ray structures have been published (Hammen et al., 1991; van Nuland et al., 1992; Jia et al., 1994).

In model peptides, the downfield-shifted amide proton of an Asn/Gln side-chain group has stereospecifically been assigned to E (*anti* to the carbonyl oxygen) and the upfield-shifted resonance to Z (*syn* to the carbonyl oxygen). These assignments cannot necessarily be assumed in proteins, where the presence of neighboring aromatic groups could affect the chemical shifts of the E and Z protons. The E and Z resonances in HPr were assigned from an H_2NCO-E COSY (Löhr and Rüterjans, 1997), which established that for all
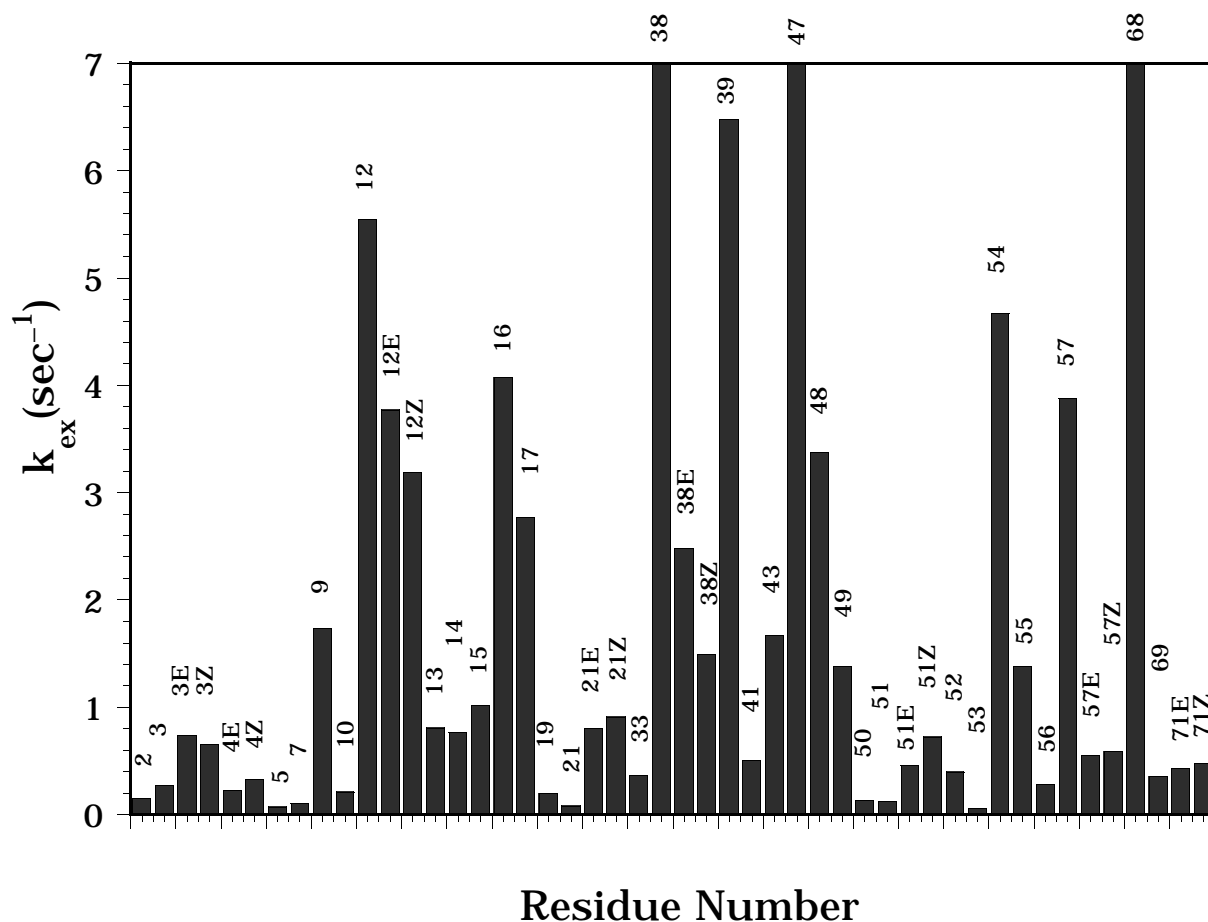
Figure 2. Histogram of solvent exchange rates (k_{ex}) in units of s^{-1} for rapidly exchanging backbone and side-chain amide protons plotted versus the amino acid sequence in HPr. The bar graph shows only those residues whose exchange rates are greater than 0.05 s^{-1}. The bars are labeled with residue number. Since the exchange rates of the backbone amide protons of Asn[38], Leu[47], and Glu[68] are greater than 30 s^{-1}, they are drawn out of scale to enable easier visualization of the remaining residues. The histogram shows that the side-chain amide groups exchange slower than some of the backbone amide protons and the exchange rates differ from one side-chain amide group to the next.

the primary amide NH_2 groups in HPr, the downfield-shifted resonances arise from the E proton (see Figures 1A and 1B).

Exchange rates of backbone and side-chain amide protons were measured using a slightly modified version of the previously published pulse sequence, where a selective inversion pulse on water is applied (Grzesiek and Bax, 1993b). A water-NOESY with a mixing time of 100 ms was acquired on uniformly ^{15}N-labeled HPr. Spectra were collected at four pH values (6.5, 7.4, 7.8, and 8.3; 25 °C) to distinguish between NOE and exchange interactions with water (Spera et al., 1991). A region of the water-NOESY difference spectrum at pH 7.4, highlighting side-chain amide resonances, is shown in Figure 1C. The spectrum illustrates the wide range of solvent exchange

behaviors exhibited by side-chain amide groups. For example, Asn[12] and Asn[38] show very strong difference peaks, whereas the difference peaks for Gln[4] and Gln[71] are very weak.

[15]N R_1 and ^{1}H spin-flip (ρ_1) relaxation rates were required to determine the pseudo-first-order rate constant, k_N for magnetization exchange between the amide protons and water (Grzesiek and Bax, 1993b). [15]N R_1 for the backbone amide protons were obtained as described previously (Farrow et al., 1994). Due to the complexity of the NH_2 spin system, [15]N T_1 for the side-chain amide protons was measured in a 50% H_2O/50% D_2O solution with the HSQC-flipback pulse sequence (Grzesiek and Bax, 1993a), modified to measure [15]N T_1s (details to be published separately). The average values of [15]N T_1 for the backbone and side-

Table 1. Solvent exchange rates (k_{ex}) for the backbone and side-chain amide protons in HPr at pH 7.4

Residue	k_{ex}[a]	Residue	k_{ex}
F2	0.15 (0.1)[b]	T52	0.40 (0.04)
Q3	0.27 (0.01)	L53	0.06 (0.01)
E5	0.07 (0.02)	G54	4.7 (0.2)
T7	0.10 (0.04)	L55	1.4 (0.6)
T9	1.7 (0.1)	T56	0.28 (0.02)
A10	0.21 (0.04)	Q57	3.9 (0.7)
N12	6 (1)	E68	33 (7)
G13	0.8 (0.1)	D69	0.36 (0.06)
L14	0.76 (0.06)	Q3E	0.7 (0.1)
H15	1.0 (0.3)	Q3Z	0.65 (0.04)
T16	4.1 (0.2)	Q4E	0.22 (0.02)
R17	2.8 (0.3)	Q4Z	0.32 (0.05)
A19	0.20 (0.03)	N12E	3.8 (0.2)
Q21	0.08 (0.4)	N12Z	3.2 (0.2)
I33	0.36 (0.02)	Q21E	0.80 (0.05)
N38	95 (15)	Q21Z	0.91 (0.1)
G39	6.5 (0.1)	N38E	2.5 (0.2)
S41	0.50 (0.04)	N38Z	1.5 (0.2)
S43	1.67 (0.08)	Q51E	0.46 (0.5)
L47	43 (15)	Q51Z	0.72 (0.06)
F48	3.4 (0.3)	Q57E	0.54 (0.03)
K49	1.4 (0.1)	Q57Z	0.59 (0.06)
L50	0.1 (0.02)	Q71E	0.43 (0.05)
Q51	0.12 (0.02)	Q71Z	0.48 (0.04)

[a] k_{ex} values are given in s^{-1}.
[b] Values given in brackets are standard errors.

Table 2. Solvent exchange rates (k_{ex}) and temperature coefficients ($\Delta\delta/\Delta T$) for the side-chain amide protons in HPr

Residue	k_{ex}[a] pH (9.0)	$\Delta\delta/\Delta T$ (ppb/K)
3E	26 (3)[b]	5.7
3Z	25 (1)	6.4
4E	8 (1)	4.3
4Z	11 (1)	7.5
12E	144 (6)	7.6
12Z	122 (4)	6.1
21E	30 (1)	−2.9
21Z	33 (3)	6.8
38E	93 (6)	6.7
38Z	55 (4)	3.2
51E	17 (1)	−1.1
51Z	27 (2)	7.5
57E	21 (1)	9.6
57Z	22 (2)	5.0
71E	16 (1)	6.1
71Z	18 (1)	7.5
GlnE	490[c]	–
GlnZ	123[c]	–
AsnE	834[c]	–
AsnZ	195[c]	–

[a] k_{ex} values are given in s^{-1}.
[b] Values given in brackets are standard errors.
[c] Exchange rates in model amino acids.

chain amide nitrogens in HPr are 400 and 580 ms, respectively. ^{1}H spin-flip rates were determined by measuring the decay rate of the $H_Z^N N_Z$ magnetization using an experiment described previously (Peng and Wagner, 1992), modified with watergate and gradients for water and artifact suppression. The decay rate of the $H_Z^N N_Z$ magnetization is a sum of ρ_1, k_N and ^{15}N R_1 for macromolecules. The decay rate was measured at the four pH values, mentioned above. The ^{15}N relaxation rates were measured at pH 6.5 and assumed to be the same at all pH values. The solvent exchange rate, k_{ex}, was computed from k_N at the four pH values, as described previously (Spera et al., 1991).

E. coli HPr has 85 residues. The backbone amide resonances of 40 residues are not visible in the first time point of an H-D exchange series, indicating that their lifetime is on the order of milliseconds to seconds. Of the 40 backbone amide resonances not visible in the first time point of an H-D exchange series, 33 have exchange rates measurable by the approach just

described. The values of ^{15}N T_1 at pH 6.5, the decay rate of the $H_Z^N N_Z$ magnetization, and k_N at the four pH values for all 33 resonances are provided as supplementary material. The value of k_{ex} at a particular pH is computed from the equation

$$k_{ex} = (k_N^{(2)} - k_N^{(1)})/(10^{\Delta pH} - 1) \qquad (1)$$

where $k_N^{(2)}$ and $k_N^{(1)}$ are the k_N values at two pH values, and ΔpH is the difference between $pH^{(2)}$ and $pH^{(1)}$. The measurements were performed at four pH values, allowing several determinations of k_{ex} at a single pH to be made. We report the mean of these values in Table 1. k_{ex} values for those backbone and side-chain amide protons that have exchange rates greater than 0.05 s^{-1} at pH 7.4 are listed.

A histogram of exchange rates versus residue number is shown in Figure 2. To our surprise, about 14 backbone amide protons in HPr exchange faster than the side-chain amide protons. The exchange rates of

the side-chain amide protons range between 0.2 to 3.8 s^{-1} at pH 7.4, 25 °C. The exchange rates of the fast exchanging backbone amide protons range from 0.06 to 95.0 s^{-1}. The only reported instance of slowly exchanging side-chain amide groups is in BPTI, where they participate in hydrogen bonds (Tüchsen and Woodward, 1987). One of the side-chain amide groups is buried and the other group is on the surface of the protein. We examined the X-ray structure of HPr to identify hydrogen bonding interactions involving the side-chain amide groups (Jia et al., 1994). The side-chain amide group of Gln^{51} is predicted to participate in a hydrogen-bond, the consequences of which will be discussed further below. We also used the program ACCESS (Lee and Richards, 1971) to calculate the surface accessibilities in both the crystal and the solution (van Nuland et al., 1992) structure of *E. coli* HPr. None of the side-chain amide groups appear to be significantly buried, although some have lower accessibility than the fastest exchanging backbone amide protons.

Solvent exchange rates of the E and Z amide protons have been measured in model amino acids, N-acetyl-Asn-N^{α}-methylamide and N-acetyl-Gln-N^{α}-methylamide (Krishna et al., 1982). In these model systems, it was shown that in a general base-catalyzed exchange reaction, the E proton exchanges about four-fold faster than the Z proton. Interpretation of solvent exchange rates in proteins is complicated by inductive effects of neighboring residues competing with solvent accessibility and participation in H-bonds. However, the relative solvent exchange rates of the E and Z protons of a particular side-chain amide group should only depend upon the presence of a hydrogen bond and/or solvent accessibility. We therefore attempted to examine the solvent exchange rates in more detail to see how the protein structure affected the behavior of E and Z protons in HPr. Measurement of the individual exchange rates of the E and Z protons is complicated in proteins because the solvent exchange rate will compete with (i) intramolecular NOE buildup between the E and Z protons and (ii) chemical exchange due to restricted rotation about the C-N bond. The rate constants for rotation about the C-N bond in small primary amide compounds in aqueous solution have been found to range between 1–10 s^{-1} (Redfield and Waelder, 1979). The NOE buildup rate has not been determined. Lowering the temperature will slow the rotation about the C-N bond, but will increase the rate of the NOE buildup. Therefore, in order to work under conditions where the solvent exchange rate is faster

than the rotational rate and the NOE buildup rate, the exchange measurements were repeated at pH 9.0 (the sample begins to precipitate at pH > 9). A mean value of k_{ex}, at pH 9.0 was computed as explained above. In order to minimize the errors induced by the effects mentioned in (i) and (ii), the k_N values at pH 6.5 were not used. The rates are reported in Table 2, which also includes the exchange rates for Asn/Gln E and Z protons at pH 9.0 in model amino acids (Krishna et al., 1982). The side-chain amide protons of Asn^{12} and Asn^{38} exchange so rapidly that their resonances are not observable at pH 9.0. Their exchange rates were therefore extrapolated to pH 9.0. Asn^{12} and Asn^{38} side-chain amide groups in HPr behave similar to the model Asn amino acid, i.e., the E protons exchange faster than the Z protons. But the difference in exchange rates between the E and Z protons is smaller than in model amino acids, suggesting that the solvent exchange rate is compromised by the NOE build up rate and the rotational rate. It is interesting to note that the solvent exchange rate of the Z proton of Asn^{12} approaches that of the model amino acid. However, the solvent exchange rates for all other side-chain amide protons in HPr are much reduced, demonstrating the influence of protein structure. The exchange behavior for the E and the Z protons of the remaining side-chain amide groups is also varied: five side-chain amide NH_2 groups have similar exchange rates for their E and Z protons within the error limits and one side-chain amide NH_2 group shows a slower exchange rate for its E proton, in contrast to the behavior observed in model amino acids.

The side-chain of Gln^{51} deviates the most from the behaviour predicted from model peptides. Its E proton exchanges appreciably slower than its Z proton (17 s^{-1} vs. 27 s^{-1}). We proceeded next to see if the decreased exchange rate could be correlated with a reduced temperature coefficient. Temperature coefficients were measured from a series of ^{1}H-^{15}N HSQC spectra collected at 15 °C, 20 °C, 25 °C, 30 °C, 38 °C and 45 °C. Chemical shifts as a function of temperature for some of the side-chain amide protons are plotted in Figure 3A. Temperature coefficients, $\Delta\delta/\Delta T$, are listed in Table 2. Figure 3B shows a histogram of the exchange rates of the side-chain amide protons at pH 9.0 (dark shaded bars) and the temperature coefficients (cross-hatched bars). Several side-chain amide protons exhibit reduced temperature coefficients. For example, 4E, 38Z, and 57Z have anomalously low temperature coefficients because their chemical shifts are close to random coil values at all temperatures
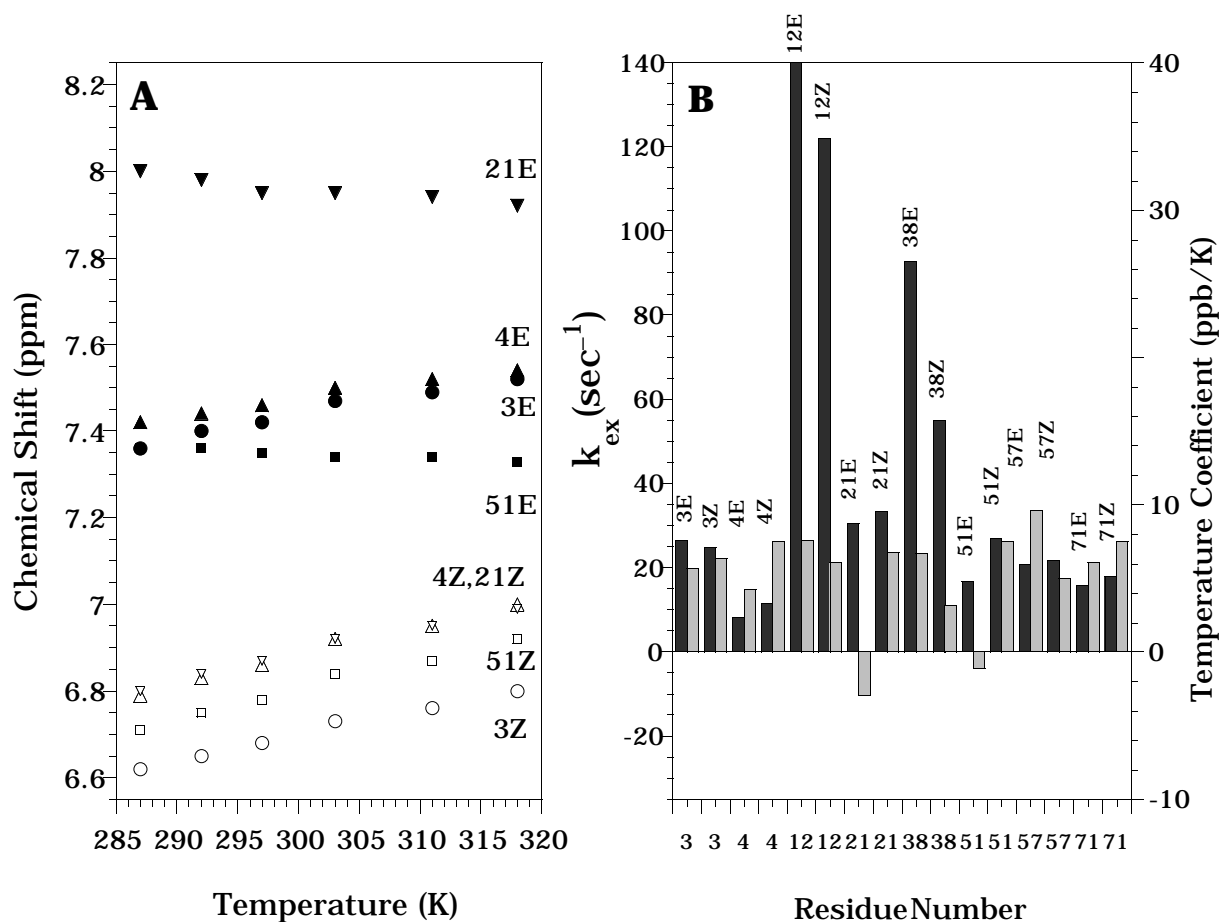
Figure 3. (A) Plots of chemical shifts (ppm) versus temperature (K) for some of the side-chain amide protons in HPr. The filled symbols represent E protons and the open symbols represent Z protons. It can be seen from the figure that the Z protons shift towards the random coil value of 6.9 ppm and the E protons shift towards the random coil value of 7.5 ppm except for Gln^{51} E. (B) Histogram of k_{ex} (s^{-1}) and temperature coefficients (ppb/K) plotted versus the primary amide NH_2 groups in HPr. The black bars represent k_{ex} and are marked with Asn/Gln residue number followed by E/Z designation. The grey bars represent temperature coefficients.

studied. The random coil positions of the E and Z protons are 7.5 ppm and 6.9 ppm, respectively. While all the other side-chain protons shift in a linear fashion towards the random coil position, the chemical shift of Gln^{51}E is essentially constant over the entire temperature range with a $\Delta\delta/\Delta T$ of –1.1 ppb/K. The chemical shift changes from 7.36 ppm at 15 °C to 7.33 ppm at 45 °C. In peptides, there is no clear correlation between reduced temperature coefficients and hydrogen bonding. However, both a reduced solvent exchange rate and a reduced temperature coefficient usually implicate participation in a hydrogen bond, as has been demonstrated recently for backbone amide protons (Baxter and Williamson, 1997).

In the crystal structure of *E. coli* HPr, the side-chain amide group of Gln^{51} appears to be hydrogen bonded to a water molecule. In a water-ROESY spectrum (Grzesiek and Bax, 1993b), protons (i) involved in an NOE interaction with water, (ii) proximal to H_α resonating close to water and (iii) proximal to hydroxyl groups will appear as negative cross peaks. Figure 4 shows the relevant region of the water-ROESY difference spectrum of HPr collected at pH 6.5, 25 °C. Only negative peaks are shown. The strong negative peaks from Ser^{43}, Ser^{46}, and Thr^{56} are due to the intra residue NOE from the hydroxyl group. The ROE cross peak from Asp^{69} is due to its H_α which resonates at 4.91 ppm. The faint ROE cross peaks from 3E, 4E, 4Z, 57E, and 57Z are either due to proximal hydroxyl protons or to proximal H_α protons. There are no hydroxyl protons or H_α protons proximal to the side chain of Gln^{51} (both X-ray and NMR structures were
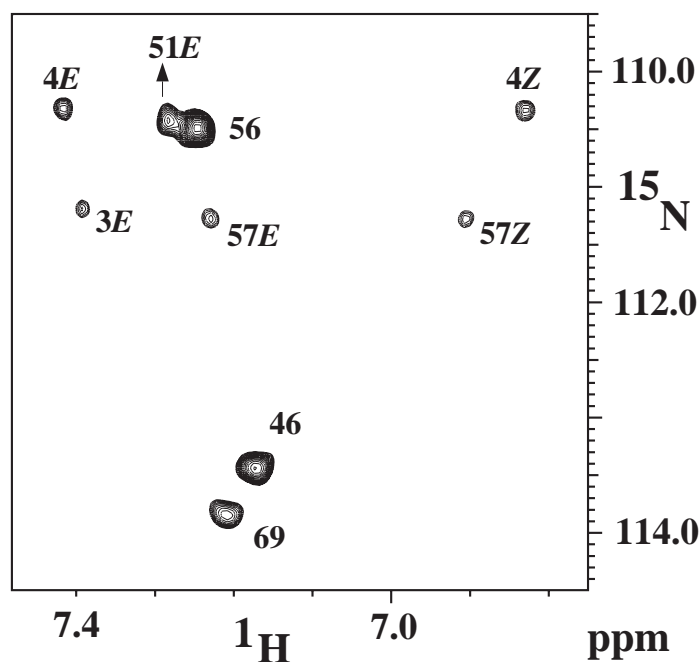
Figure 4. A region of the water-ROESY difference spectrum showing the primary amide NH$_2$ region of HPr. The spectrum was collected at pH 6.5 and at 30 °C on a 0.5 mM HPr sample with 64 scans per complex t$_1$ point. The ROESY mixing time used was 25 ms. The remaining experimental parameters are the same as in Figure 1. Only negative/ROE peaks are shown. Cross peaks are indicated with backbone and side-chain amide residue number. The arrow points to the label 51E. The ROE cross peaks can arise from different sources of cross-relaxation and are explained in the text.

examined). Hence, the ROE peak observed for Gln^{51}E confirms that an interaction between the Gln^{51} side-chain and a water molecule observed in the crystal is also present in solution.

The temperature coefficient of 21E is much lower than that of 21Z – 2.9 ppb/K versus 6.8 ppb/K. However, the solvent exchange rates for the E and the Z protons are the same within the limits of error. There are two reasons for this apparent anomaly. One is that a lowered temperature coefficient does not necessarily imply a reduced exchange rate. The second is that the intra-proton NOE and rotation about the C-N bond compromise the extraction of individual E and Z exchange rates. The degree to which these processes affect the measurement of solvent exchange rates varies from one side chain amide group to another (P. Rajagopal and R.E. Klevit, unpublished observation). Work is in progress to devise alternative strategies to obtain values of k$_{ex}$ uncompromised by these processes. It remains to be seen then if a better correlation can be obtained between temperature coefficients and pure E/Z solvent exchange rates.

In conclusion, useful and interesting information can be obtained by investigating side-chain solvent exchange rates. In this report, we have shown that side-chain amide exchange rates can vary significantly from one side-chain amide group to another and that H-bonds and interactions with bound water can be well defined. We believe that these measurements will be a useful probe for defining interactions at the intermolecular interface.

References

Bai, Y., Milne, J.S., Mayne, L. and Englander, S.W. (1993) *Proteins Struct. Funct. Genet.*, **17**, 75–86.

Delaglio, F. , Grzesiek, S., Vuister, G., Zhu, G., Pfeifer, J. and Bax, A. (1995) *J. Biomol. NMR*, **6**, 277–293.

Baxter, N.J. and Williamson, M.P. (1997) *J. Biomol. NMR*, **9**, 359–369.

Farrow, N.A., Muhandiram, R., Singer, A.U., Pascal, S.M., Kay, C.M., Gish, G., Shoelson, S.E., Pawson, T., Forman-Kay, J.D. and Kay, L.E. (1994) *Biochemistry*, **33**, 5984–6003.

Garrett, D.S., Powers, R., Gronenborn, A.N. and Clore, G.M. (1991) *J. Magn. Reson.*, **95**, 214–220.

Grzesiek, S. and Bax, A. (1993a) *J. Am. Chem. Soc.*, **115**, 12593–12594.

Grzesiek, S. and Bax, A. (1993b) *J. Biomol. NMR*, **3**, 627–638.

Hammen, P.K., Waygood, E.B. and Klevit, R.E. (1991) *Biochemistry*, **30**, 11842–11850.

Jia, Z., Van Donselaer, M., Hengstenberg, W., Quail, J.W. and Delbaere, L.T. (1994) *J. Mol. Biol.*, **236**, 1341–1355.

Krishna, N.R., Sarathy, K.P., Huang, D.H., Stephens, R.L., Glickson, J.D., Smith, C.W. and Walter, R. (1982) *J. Am. Chem. Soc.*, **104**, 5051–5053.

Lee, B. and Richards, F.M. (1971) *J. Mol. Biol.*, **55**, 379–400.

Löhr, F. and Rüterjans, H. (1997) *J. Magn. Reson.*, **124**, 255–258.

Narutis, V.P. and Kopple, K.D. (1983) *Biochemistry*, **22**, 6233–6239.

O'Neil, J.D.J. and Sykes, B.D. (1989) *Biochemistry*, **28**, 6736–6745.

Peng, J.W. and Wagner, G. (1992) *J. Magn. Reson.*, **98**, 308–332.

Rajagopal, P. and Klevit, R.E. (1994) *Tech. Protein Chem.*, **5**, 439–445.

Redfield, A.G. and Waelder, S. (1979) *J. Am. Chem. Soc.*, **101**, 6151–6162.

Spera, S., Ikura, M. and Bax, A. (1991) *J. Biomol. NMR*, **1**, 155–165.

Tüchsen, E. and Woodward, C. (1987) *Biochemistry*, **26**, 8073–8078.

van Nuland, N.A.J., Grotzinger, J., Dijkstra, K., Scheek, R.M. and Robillard, G.T. (1992) *Eur. J. Biochem.*, **210**, 881–891.

Wüthrich, K. and Wagner, G. (1979) *J. Mol. Biol.*, **130**, 1–18.